Applied Catalysis B: Environmental 100 (2010) 1–9

Contents lists available at ScienceDirect

Applied Catalysis B: Environmental

journal homepage: www.elsevier.com/locate/apcatb

Review

Immobilization of halogenated porphyrins and their copper complexes in MCM-41: Environmentally friendly photocatalysts for the degradation of pesticides

M. Silva[a], M.E. Azenha[a,*], M.M. Pereira[a,*], H.D. Burrows[a], M. Sarakha[b,*], C. Forano[c], M.F. Ribeiro[d], A. Fernandes[d]

[a] Department of Chemistry, Faculty of Sciences and Technology, Coimbra University, Rua Larga, 3004-535 Coimbra, Portugal
[b] Laboratoire de Photochimie Moléculaire et Macromoléculaire, UMR CNRS 6505, Université Blaise Pascal, F-63177 Aubière Cedex, France
[c] Laboratoire des Matériaux Inorganiques, UMR CNRS 602, Université Blaise Pascal, F-63177 Aubière Cedex, France
[d] Department of Chemical Engineering, IST, Lisbon Technical University, Av. Rovisco Pais, 1100-054 Lisboa, Portugal

ARTICLE INFO

Article history:
Received 19 May 2010
Received in revised form 21 July 2010
Accepted 28 July 2010
Available online 12 August 2010

Keywords:
Porphyrins
Immobilization
MCM-41
Pesticides photodegradation
Radical mechanism

ABSTRACT

MCM-41 immobilized (*ship-in-a-bottle*) *meso*-tetrakis(2-fluorophenyl)porphyrin, TFPP@MCM-41, and *meso*-tetrakis(2,6-dichlorophenyl)porphyrin, TDCPP@MCM-41, and the corresponding copper metal complexes, CuTFPP@MCM-41 and CuTDCPP@MCM-41, were successfully synthesized by the condensation of pyrrole with the desired benzaldehydes, using the nitrobenzene method, in the absence or presence of copper salt, respectively. Their characterization was performed by DRS-UV–vis, luminescence, EPR, ATR-FTIR spectroscopies, PXRD, TG/DTA, nitrogen adsorption analysis and elemental analysis.

All the immobilized porphyrins TFPP@MCM-41, TDCPP@MCM-41, CuTFPP@MCM-41 and CuTDCPP@MCM-41 were tested in the photodegradation of 2,4,6-trimethylphenol and TFPP@MCM-41 showed the best performance. The studies were extended to the photodegradation of pesticides fenamiphos and diuron using TFPP@MCM-41 as photocatalyst and the photoproducts were identified by LC–MS. Mechanistic studies, using furfuryl alcohol as singlet oxygen trap revealed that there was no involvement of this species in the photodegradation of the above mentioned pesticides and the identified photoproducts are consistent with a radical mechanism.

An efficient photolysis of the pesticides after 5 h, in aerated aqueous solutions, was observed with TFPP@MCM-41 with no loss of the photocatalytic activity over recycling. These heterogeneous photocatalysts with no significant decomposition of the porphyrin make them promising candidates for water treatment.

Contents

* Corresponding authors. Tel.: +351 239854465; fax: +351 239827703.
E-mail addresses: meazenha@ci.uc.pt (M.E. Azenha), mmpereira@qui.uc.pt (M.M. Pereira), mohamed.sarakha@univ-bpclermont.fr (M. Sarakha).

0926-3373/$ – see front matter © 2010 Elsevier B.V. All rights reserved.
doi:10.1016/j.apcatb.2010.07.033

1. Introduction

The photodecomposition of organic pesticides is of significance, both from the environmental point of view and for the development of new, safer, and more effective pesticides and formulations [1]. Photochemical investigation of corresponding homogeneous and heterogeneous systems constitutes a source of considerable interest for the transformation, mineralization and elimination of chemicals from different environmental compartments. Many of these chemicals, when they are present in aqueous media, can undergo photochemical transformation with sunlight *via* direct or/and indirect photoreactions. Advanced oxidation processes (AOPs) are considered to have great relevance in environmental applications. They can be used as water remediation techniques, frequently leading to the mineralization of organic pollutants through the reaction with highly oxidizing species, such as hydroxyl radicals [2–5]. Heterogeneous photocatalysis involving metal oxide semiconductors, such as TiO_2 and ZnO, has proven to be one of the most powerful techniques for complete degradation of persistent pesticides [6,7]. However, there is complementary interest in the development of other techniques for pesticide degradation, such as those involving electrogenerated Fenton reagent [8], biodegradation [9], X-ray irradiation [10], and combined degradation using both semiconductors and organic sensitizers [11,12].

Over the last decades much effort has been devoted to the development of new homogeneous photocatalysts based on porphyrins and metalloporphyrins, because these may lead to new, more selective and "cleaner" processes, with applications in various areas [13–17], particularly in the photodegradation of pollutants [18–21].

Metalloporphyrins present some disadvantages as homogeneous catalysts, including poor stability and limited reuse. One simple strategy to overcome these drawbacks consists of immobilizing metalloporphyrins with suitable insoluble supports. Different inorganic host materials have been used and include modified silica surfaces [22–24], organic polymers [25–27], zeolites and clays [28–30]. Ordered mesoporous silicas represent another class of supports that have been extensively studied since these particular materials present some important advantages, in particular their enlarged porous systems that allow incorporation of larger molecules [30,31]. The immobilization of organic moieties can be made using different synthetic strategies [31,32], including encapsulation [33], ion exchange [34–36], covalent bonding [37], inorganic support post-modifications [38], etc.

To the best of our knowledge, the use of metalloporphyrins immobilized into mesoporous materials for pesticide photodegradation applications, recently presented in a preliminary report by some of us, has not been yet significantly exploited [39]. In this paper we describe the immobilization of *meso*-tetrakis(2-fluorophenyl)porphyrin (TFPP), *meso*-tetrakis(2,6-dichlorophenyl)porphyrin (TDCPP) and their copper complexes, CuTFPP and CuTDCPP, within MCM-41 mesoporous molecular sieve, using *in situ* porphyrin synthesis (*ship-in-a-bottle*) with nitrobenzene methodology [40,41]. Some structural characterization of immobilized metalloporphyrins have been made using combined DRS-UV–vis absorption, luminescence, electron paramagnetic resonance (EPR), attenuated total reflectance Fourier transform infrared (ATR-FTIR) spectroscopies, powder X-ray diffraction (PXRD), thermogravimetric/differential thermal analysis (TG/DTA) and nitrogen adsorption measurements. The immobilized porphyrins and metalloporphyrins have been tested as photocatalysts for photodegradation of pesticides, specifically 2,4,6-trimethylphenol (**1**), fenamiphos (**2**) and diuron (**3**).

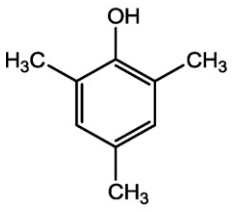

1

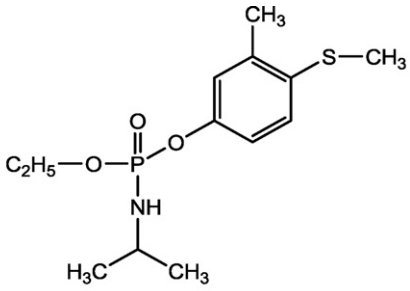

2

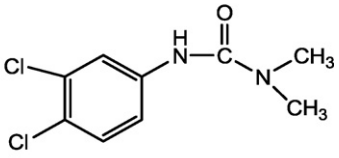

3

2. Experimental

2.1. Materials

2,4,6-Trimethylphenol (99.5%), fenamiphos (99.9% purity) and diuron (>98%) were obtained from Aldrich and were used without any further purification. Furfuryl alcohol ((2-hydroxymethyl)furan, >98%) was purchased from Fluka. All other chemicals and solvents were of the purest grade commercially available and were used as received. All aqueous solutions were prepared with ultrapure water obtained from an ultrapure water system having a resistivity >18 MΩ cm^{-1}. The MCM-41, pyrrole and substituted benzaldehyde were purchased from Aldrich, and pre-treated at 500 °C for 18 h in an oven. Copper acetate monohydrate (> 97%) was obtained from Fluka.

2.2. Preparation of immobilized porphyrins

The immobilized porphyrins (TFPP@MCM-41 and TDCPP@MCM-41) used in all the experiments were prepared accord-

ing to the previously described *ship-in-a-bottle* procedure [28]. The copper porphyrins (CuTFPP@MCM-41 and CuTDCPP@MCM-41) were obtained by mixing 2.0 g of MCM-41 and 0.5 g (2.5 mmol) of copper(II) acetate monohydrate in 140 mL of glacial acetic acid and 93 mL of nitrobenzene. To this mixture the corresponding substituted benzaldehydes (9.5×10^{-3} mol) were added. The temperature was increased to 120 °C and the pyrrole was slowly added (9.5×10^{-3} mol). The reaction continued for 2 h. At the end, all the materials were filtered and Soxhlet extracted sequentially with CH_2Cl_2, CH_3CN and $CHCl_3$, until no porphyrin or precursors were detected in the solution, by UV–vis spectroscopy (~72 h). The resulting immobilized sensitizers were dried overnight at 100 °C.

2.3. Instrumentation

UV–vis absorption spectra of solution samples were measured on a Shimadzu UV-2010 double-beam spectrometer over the range 200–800 nm. DRS-UV–vis absorption spectra of solid samples were done on a Shimadzu UV-2450 double-beam spectrometer with an integrating sphere over the range 300–800 nm. Luminescence spectra were obtained on a SPEX Fluorolog 3-22 spectrophotometer, using a 300 W xenon arc lamp as excitation source. The luminescence spectra on solid samples were measured using a specially designed metal support with a quartz window. Attenuated total reflectance Fourier transform infrared (ATR-FTIR) spectra were measured over the range 400–4000 cm^{-1} on a FTIR Nicolet 5700 (ThermoElectron Corporation) spectrometer equipped with a Smart Orbit accessory. The electron paramagnetic resonance (EPR) spectra were obtained using a Bruker EMX spectrometer. Microwave frequencies were measured with an X-band microwave Bridge (ER641XG). The *g* values were standardized using DPPH (1,1′-diphenyl-2-picrylhydrazyl) as a reference. Thermogravimetric/differential thermal analysis (TG/DTA) were obtained using a Setaram TG–DTA92 thermogravimetric analyzer coupled with a mass spectrometry analyzer (Thermostar 300 Balzers Instruments) in the temperature range of 25–1050 °C, with a heating rate of 5 °C min^{-1}, under air flow in an alumina crucible. Powder X-ray diffraction (PXRD) patterns of solids were recorded using Philips X-Pert Pro diffractometer equipped with a graphite monochromator using Cu Kα radiation (λ = 0.15415 nm). Patterns were recorded over the 2–70° (2θ) range in steps of 0.0334° with a counting time per step of 30 s. Nitrogen adsorption measurements were carried out with a Micromeritics ASAP 2020 surface area and porosity analyzer. Prior to analysis, all samples were pre-treated for 10 h at 80 °C under vacuum. The BET surface areas were determined for the low-pressure region (p/p_0 < 0.26). The mesopore volumes and pore size distributions were calculated using the BJH model.

The copper and aluminium content were evaluated by inductively coupled plasma-optical emission spectrometry (ICP-OES) done in a Optima 2000 DV, Perkin Elmer; the silicium was by AAS (atomic absorption spectrometry) in a Analyst 300, Perkin Elmer; and the other elements were obtained by EA (elemental analysis) in a EA 1108 (CHNS-O), Fisons Instruments.

HPLC analysis was performed using a Millenium system equipped with a photodiode array detector (DAD). The detection wavelength was set at 220 nm or 280 nm for the pesticides. The elution was accomplished by using a reverse phase C8, Agilent XDB column (250 mm × 4.5 mm i.d., 5 μm) and with water (0.1% formic acid) and methanol (3/7 by volume). The flow rate was 1.0 mL min^{-1} and an injection volume of 50 μL was used.

LC–MS studies were carried out with Q-TOF-Micro/water 2699 from CRMP centre at the University Blaise Pascal. This is equipped with an electrospray ionisation source (ESI) and a Waters photodiode array detector. Each single experiment permitted the simultaneous recording of both UV chromatogram at a pre-selected wavelength and an ESI-MS full scan. Data acquisition and processing were performed by MassLynx NT 3.5 system. Chromatography was run using a Nucleosil column 100-5 C18 ec (250 mm × 4.6 mm, 5 μm). Samples (5–10 μL) were injected either directly or after evaporation of the solvent for better detection. A gradient program (Table 1) was used by employing water with 0.4 vol.% acetic acid (A) and acetonitrile (B) at 1 mL min^{-1}.

Table 1
LC–MS conditions used in the gradient program.

	Time (min)			
	Initial	3	20	30
% A	95	80	5	95
% B	5	20	95	5

2.4. Irradiation set-up

Photocatalytic experiments were carried out at room temperature using a laboratory-built photoreactor consisting of six 15 W Philips TLD lamps. The reactions were carried out in a 50 mL flask, open on the top to allow entrance of air or other gases. For the photocatalytic experiments, 25 mL of substrate solution and 25 mg of catalyst were mixed. The pH of the sample solution was pH ≈ 6. The solutions were freshly prepared and kept in the dark prior to use. The initial concentration of substrate in all experiments was 1.1×10^{-4} mol L^{-1}. Before irradiation, a photocatalyst suspension containing the pesticide was allowed to equilibrate for 60 min in the dark. The adsorption of pesticide onto the catalyst surface was negligible (<1% adsorption). The solutions were irradiated with polychromatic light within the range 300–460 nm (λ_{max} = 366 nm) for 6 or 8 h. Aliquots were taken at regular periods of time (0, 30, 60, 90, 120, 180, 240, 300, 360, 420 and 480 min) from the irradiated solution and were centrifuged twice. Both the disappearance of the substrate and formation of the products were monitored by HPLC. The final supernatant was collected and analysed by HPLC/DAD. Degradation products were identified by LC–MS without any extraction or pre-concentration procedures.

3. Results and discussion

3.1. Ship-in-a-bottle synthesis of porphyrins and their copper complexes

Mesoporous (MCM-41) is an attractive and stable structure to host sensitizers, with porphyrins being good candidates [30,34,39,42]. Recently, we have described an efficient method for the *ship-in-a-bottle* synthesis of 5,10,15,20-tetrakis(2-fluorophenyl)porphyrin (TFPP) in MCM-41 [39] and its catalytic evaluation. It is well established that the structure of the porphyrins can have a significant effect on the mechanism and activity of the photocatalysts [43,44]. In this paper we enlarge our studies to the *ship-in-a-bottle* synthesis of 5,10,15,20-tetrakis(2,6-dichlorophenyl)porphyrin (TDCPP@MCM-41) and their copper complexes, CuTFPP@MCM-41 and CuTDCPP@MCM-41, in order to evaluate their performance as heterogeneous photosensitizers in the degradation of pesticides, fenamiphos and diuron. The mixture of equimolar amounts of pyrrole and aromatic aldehydes (2-fluorbenzaldehyde or 2,6-dichlorobenzaldehyde), dissolved in acetic acid–nitrobenzene (7/3), and the solid MCM-41 (2 g) were heated at 120 °C, during 2 h. After filtration, the desired porphyrins encapsulated in the cavity of MCM-41 were obtained and the supernatant solution corresponding to the free bases, TFPP and TDCPP, were recovered with 1.2 and 1.8% yields, respectively. When the synthesis was performed in the presence of copper(II) acetate, the corresponding metalloporphyrins were obtained, concomitantly

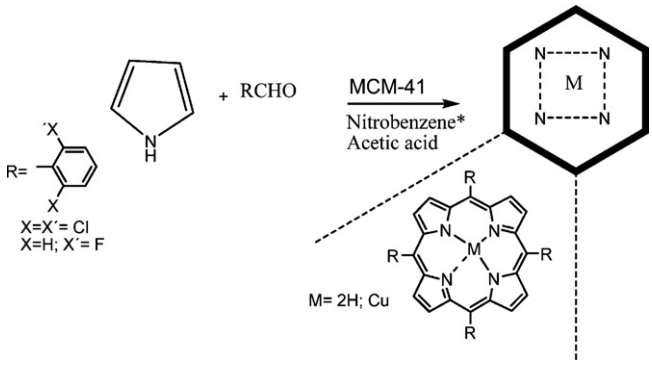

Fig. 1. Reaction scheme for the *ship-in-a-bottle* porphyrin synthesis using nitrobenzene method [39]. *For metalloporphyrin synthesis the reaction was carried out in the presence of an excess of copper(II) acetate.

with the CuTFPP and CuTDCPP in solution (2.1 and 2.5%, respectively). The proposed mechanism of synthesis is shown in Fig. 1. It should also be emphasized that, as has previously been shown for porphyrin synthesis using the nitrobenzene method in solution [40,41,45], we did not observe any contamination with the corresponding chlorins. This represents a great advantage over all the previously described *ship-in-a-bottle* porphyrin synthesis, using exclusively acetic or propionic acid as solvent [46,47].

3.2. Characterization of the immobilized porphyrins and copper porphyrins

3.2.1. DRS-UV–vis absorption spectra and luminescence spectroscopy

The UV–vis absorption of the supernatant and luminescence spectra of the CuTFPP and CuTDCPP obtained after cyclization–oxidation reaction in the presence of MCM-41 showed the characteristic bands of a copper(II) porphyrin [48]. The characteristic Soret and Q bands were observed at 415, 540 and 615–620 nm. In contrast, the electronic spectra of the TFPP@MCM-41 and TDCPP@MCM-41 synthesis supernatant presented the characteristic bands of the free base porphyrin (418, 515, 550, 594, 650 nm) [39].

Fig. 2 presents DRS-UV–vis absorption spectra of the solids MCM-41, TFPP@MCM-41 and CuTFPP@MCM-41. From analysis of the spectra we observed a slight blue shift in the Soret band with the complexation and a different maximum if the porphyrins are

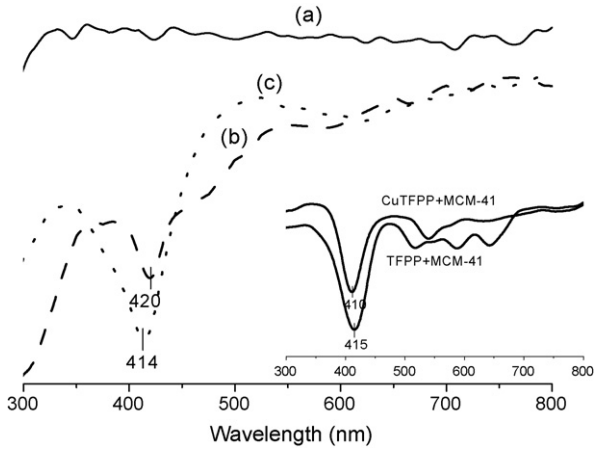

Fig. 2. DRS-UV–vis absorption spectra of the (a) MCM-41, (b) TFPP@MCM-41 and (c) CuTFPP@MCM-41. Insert spectra: TFPP and CuTFPP mechanically mixed with MCM-41.

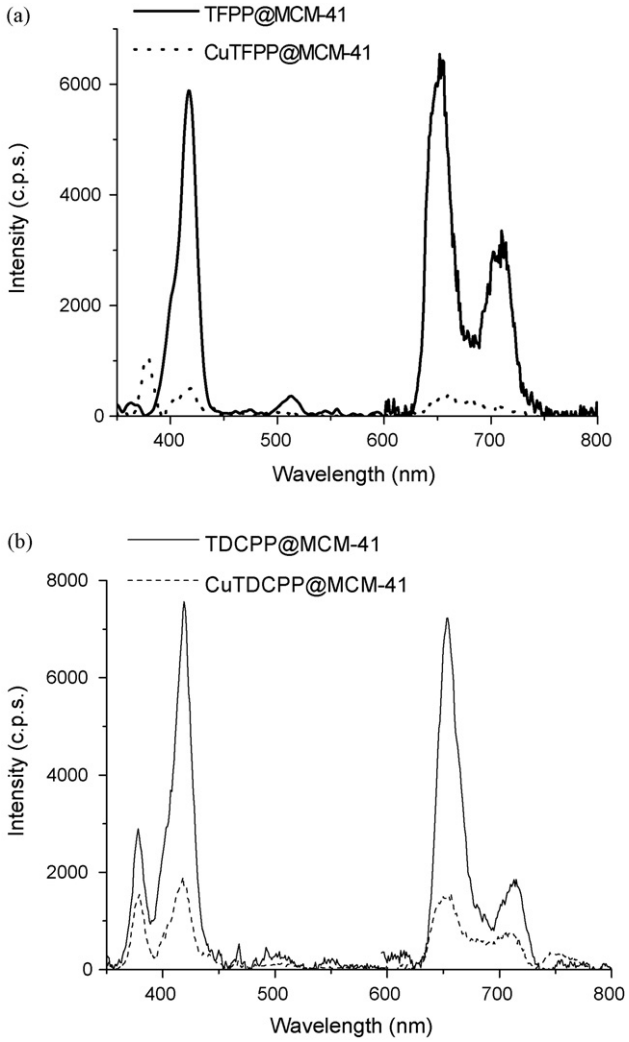

Fig. 3. Emission and excitation spectra of the (a) TFPP@MCM-41 and CuTFPP@MCM-41; (b) TDCPP@MCM-41 and CuTDCPP@MCM-41.

immobilized (inset). However, there were no signs of aggregation of the porphyrin.

The luminescence spectra of TFPP@MCM-41 and TDCPP@MCM-41 show two bands at 655 and 710 nm (Fig. 3). With CuTFPP@MCM-41 and CuTDCPP@MCM-41 these two bands have a much lower intensity making the determination of the band maxima difficult.

Whilst, as in related systems, the fluorescence spectra may result from the presence of a small amount of free base porphyrin formed through demetallation [49], they are also fully consistent with the weak fluorescence previously reported for the copper(II) porphyrins [50]. This is in agreement with the short singlet state lifetime for copper(II) porphyrins [51]. Although this may limit the efficiency of sensitized processes (bimolecular singlet excited state processes), these are still possible through the lowest triplet state or contact charge-transfer species.

3.2.2. EPR analysis

EPR spectra were observed for the MCM-41 immobilized copper(II) porphyrins. The EPR data at 77 K showed anisotropic spectra, with g values similar to those for free copper(II) complexes and characteristic of Cu^{2+} ($3d^9$ configuration, spin = 1/2). However, the spectra were not identical to those for copper(II) acetate [52] and are very different from those expected for free copper ions adsorbed in MCM-41, strongly supporting the implications of the fluorescence results that CuTFPP is present within the MCM-41. Fig. 4a

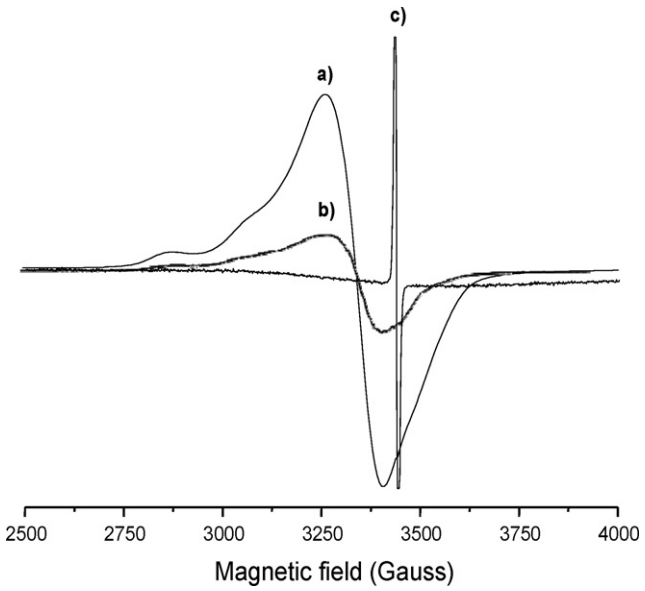

Fig. 4. X-band EPR spectra of (a) CuTFPP, (b) CuTFPP@MCM-41, (c) TFPP and DPPH at 77 K.

shows the EPR signal of CuTFPP which exhibit $g_{\perp}$ and $g_{||}$ values but no hyperfine structure due to exchange interactions. For the immobilized sample, Fig. 4b, the Cu(II) parameters observed are $g_o = 2.37$, $g_{\perp} = 2.08$ and $A_o = 126$ G. These are different from the literature EPR parameters for the free CuTPP dichloromethane solution [51]. The g_o tensor is smaller and the A_o is larger. These differences indicate that there is a greater constraint on the copper porphyrins inside the pores of MCM-41. The band in Fig. 4c corresponds to that of the DPPH reference since TFPP has no EPR signal.

3.2.3. ATR-FTIR analysis

Infrared spectra were measured on the solid samples using ATR (Fig. 5), and confirm the presence of CuTFPP immobilized into the mesoporous silica phase. Typical vibrational bands of $Si–O^-$ are observed at 1078 cm^{-1} (ν_{as} (SiO_4^-)). This is a characteristic infrared feature of MCM-41. The vibrational bands attributed to the C–H, C–C and C–N bonds of the aromatic rings are discernible in the range 1650–1350 cm^{-1} but it is difficult to give precise values because of very low intensities due to a low loading of the macrocycle into the inorganic matrix.

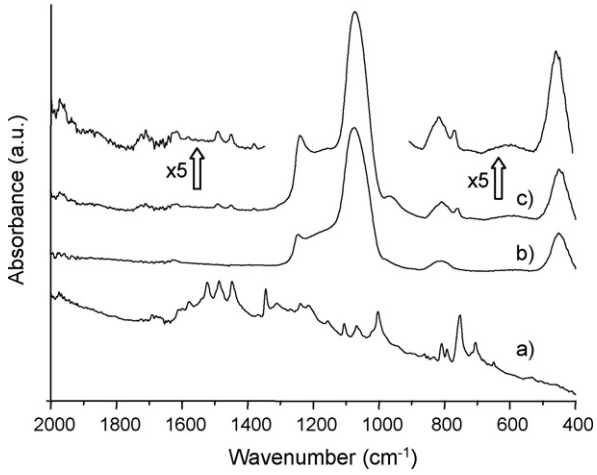

Fig. 5. ATR-FTIR spectra of (a) CuTFPP, (b) MCM-41 and (c) CuTFPP@MCM-41.

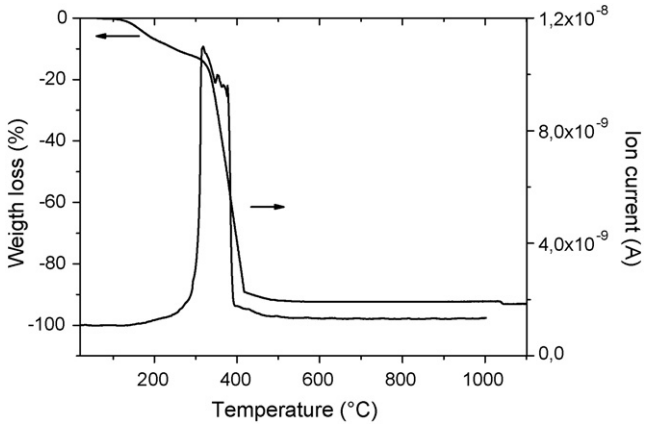

Fig. 6. Thermogram of CuTFPP.

3.2.4. Thermogravimetric analysis

The amount of copper porphyrin incorporated into MCM-41 was quantified using thermogravimetric analysis coupled with mass spectrometry of evolved gases. From TG, DTA and CO_2 mass signals, we observed that CuTFPP (Fig. 6) and CuTFPP immobilized at MCM-41 (Fig. 7) start to decompose around 280 °C. By comparison of the weight losses in the two cases, it is found that 21.5% of CuTFPP can be incorporated into the mesoporous solid. The strong interactions between the metalloporphyrin and the host structure lead to a 50 °C increase in the temperature of maximum decomposition rate which shifts from 375 °C for the free CuTFPP to 425 °C for CuTFPP@MCM-41. This, coupled with the high degree of loading, strongly supports the idea that the macromolecule is not simply adsorbed at the surface of the solid but is, in fact, encapsulated within the channels of the MCM-41 matrix.

3.2.5. Powder X-ray diffraction and nitrogen adsorption analysis

The X-ray diffractogram of CuTFPP@MCM-41 and TFPP@MCM-41 were obtained (Fig. 8), and display the same characteristic diffraction lines of the MCM-41 hexagonal array. The (1 1 0), (2 0 0) and (2 1 0) reflections are observed at 3.919°, 4.487° and 5.891° (2θ) respectively, corresponding to a d_{001} distance of 3.935 nm. No change in the position of these peaks is seen, confirming that the structure of the mesoporous MCM-41 network is retained during the *in situ* formation of CuTFPP. However, the increase of the peak widths indicates a clear effect of the synthesis upon the degree of crystallinity of the phase, as already indicated in related systems [34], and shows that *in situ* formation of CuTFPP within the MCM-

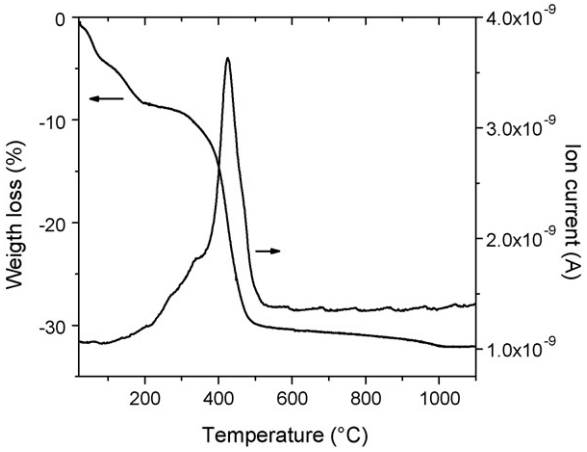

Fig. 7. Thermogram of CuTFPP@MCM-41.

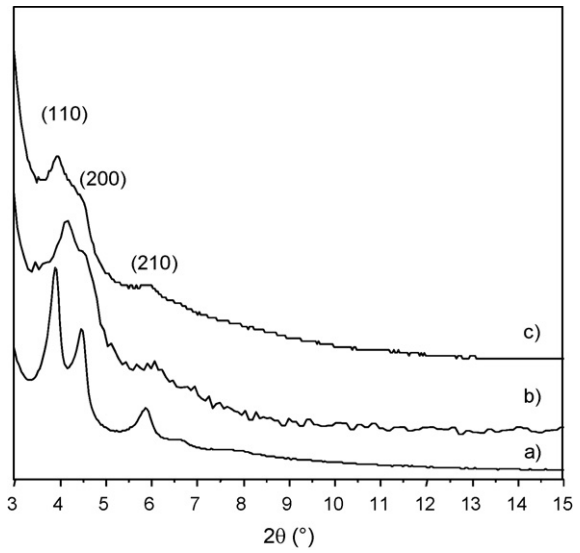

Fig. 8. X-ray diffractograms of (a) MCM-41, (b) TFPP@MCM-41 and (c) CuTFPP@MCM-41.

41 pores leads to a more amorphous character of the host structure. Indeed metallation of TFPP by Cu^{2+} ion does not induce any structural change as the porphyrin ligand impose the templating effect.

This is supported by the changes observed in surface and porosity properties of the CuTFPP@MCM-41 material compared with the support MCM-41. Both, MCM-41 and CuTFPP@MCM-41 samples, display a typical type IV N_2 adsorption isotherm characteristic of mesoporous solids (Fig. 9) with filling of mesopores commencing at $p/p_0 = 0.33$ during the adsorption phase. The net decrease (35%) of the surface area from MCM-41 to CuTFPP@MCM-41 (Table 2) provides clear evidence for the incorporation of the photocatalyst within the channels of the mesoporous silica network. This strong modification is simultaneous with the loss of the pore volume and the decrease of the pore size as shown by the pore size distribution curves. A similar behaviour was observed for the others materials.

3.2.6. Elemental analysis

The following values were obtained for elemental analysis of CuTFPP@MCM-41: Si 27%; Al 0.7%; Cu 1.1%; N 1.7%; C 17.4%; and H < 2.0%. From these, the calculated amount of copper porphyrin (CuTFPP) present in MCM-41 is 1.7×10^{-4} mol per gram of catalyst, while that of free porphyrin is 2.3×10^{-4} mol per gram of catalyst.

3.3. Photocatalytic studies

3.3.1. Photoinduced degradation of TMP

To compare the photocatalytic efficiency of the different immobilized sensitizers, described above, 2,4,6-trimethylphenol (TMP) was used as a model substrate. The degradation of TMP (1×10^{-4} mol L^{-1}) was performed by excitation with a broad band UV light ($\lambda_{max} = 366$ nm) in the presence of the photocatalysts (1–4) (at a concentration of 1.0 g L^{-1}). The kinetic profiles for the disappearance of TMP using the immobilized

Table 2
Textural parameters.

Materials	S_{BET} ($m^2\ g^{-1}$)	Pore volume (mL g^{-1})
MCM-41	1281	1.290
TFPP@MCM-41	540	0.294
CuTFPP@MCM-41	838	0.306
TDCPP@MCM-41	802	0.408
CuTDCPP@MCM-41	816	0.420

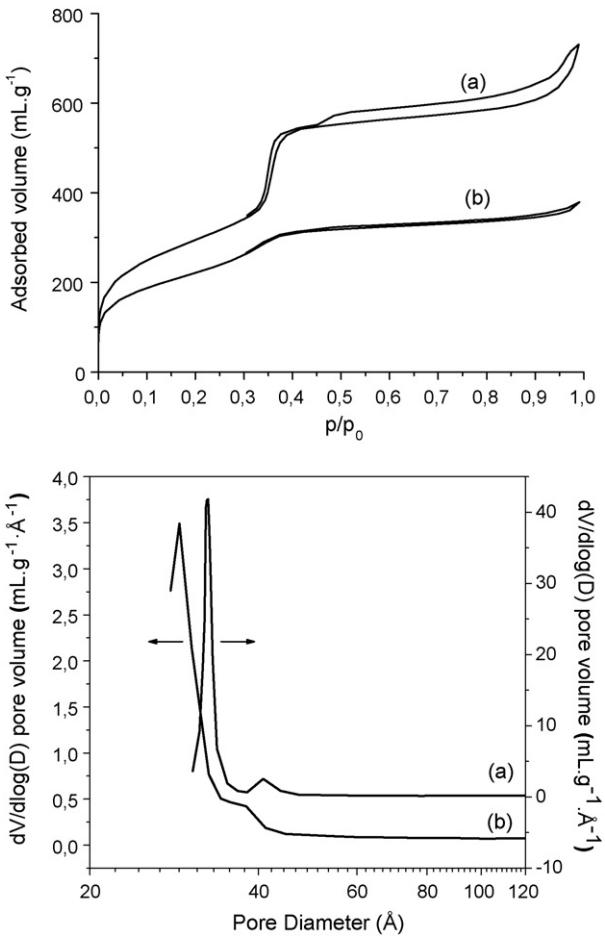

Fig. 9. Specific surface area and pore volume distribution for (a) MCM-41 and (b) CuTFPP@MCM-41.

photosensitizers (1–4) are represented in Fig. 10. It can clearly be seen that all the immobilized photocatalysts studied induce the photodegradation of TMP, but the degradation rate clearly depends from the structure of the sensitizer. The disappearance of TMP, in all cases, can be fitted by pseudo-first-order kinetics, with TFPP@MCM-41 being the most efficient photosensitizer. The observed rate constants follow the order $k_{TFPP@MCM-41} > k_{TDCPP@MCM-41} > k_{CuTFPP@MCM-41} \approx k_{CuTDCPP@MCM-41}$, showing decreased photocatalytic activity with the copper metal complexes. It should also be emphasized that under the same

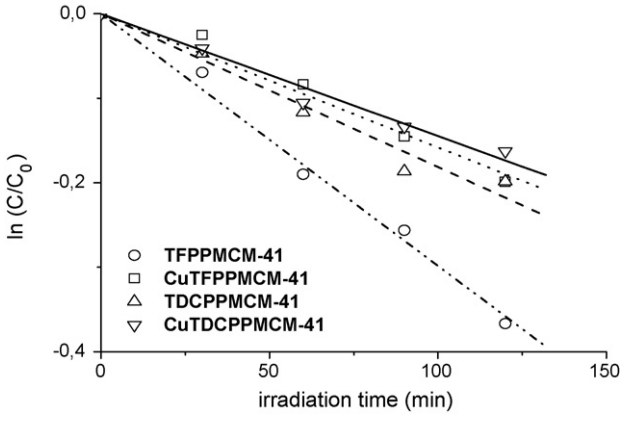

Fig. 10. Kinetics of photocatalytic degradation of TMP (pH ≈ 6) with the immobilized photocatalysts 1–4.

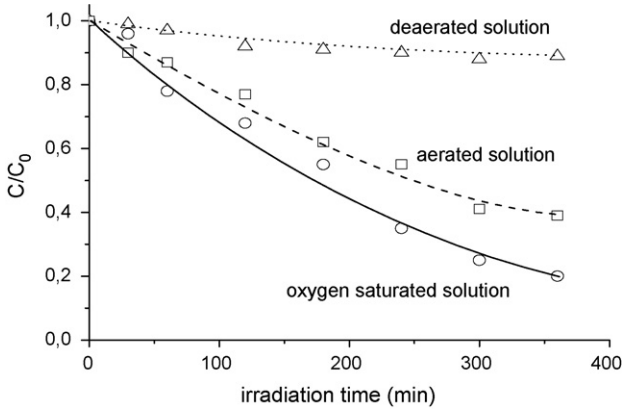

Fig. 11. Kinetics of fenamiphos photodegradation using TFPP@MCM-41 as sensitizes function of oxygen concentration.

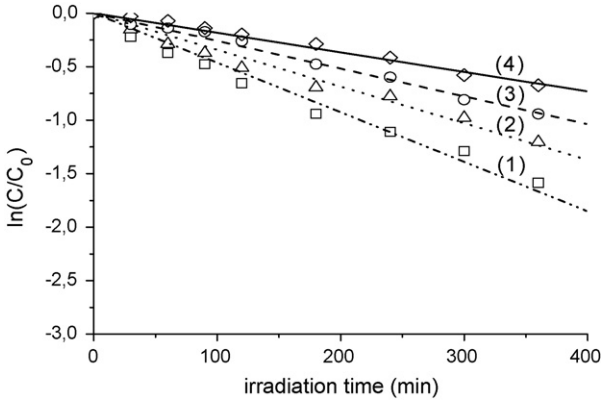

Fig. 12. Photocatalytic degradation of fenamiphos in the presence of TFPP@MCM-41 at concentrations of 3.0 (**1**), 1.5 (**2**), 1.0 (**3**) and 0.5 g L^{-1} (**4**).

experimental conditions no significant disappearance of TMP was observed by direct photolysis in the absence of the photosensitizer.

Since many photosensitized reactions using porphyrins involve singlet oxygen species [2,13], we undertook experiments to test the involvement of this type of mechanism in the photodegradation of TMP using TFPP@MCM-41 as sensitizer. These experiments were performed using furfuryl alcohol (FA) as oxygen trap. An aerated solution of TFPP@MCM-41 (1.0 g L^{-1}) and TMP (1×10^{-4} mol L^{-1}) was irradiated with UV light (polychromatic light between 300 and 460 nm, with λ_{max} = 366 nm) in the presence of FA at the concentration of (1×10^{-2} mol L^{-1}) and no significant changes on the rate constant of the disappearance of TMP were observed. Furthermore, in order to check whether $^1O_2$ is really present in these photodegradative processes, an indirect chemical method was used involving the trapping of $^1O_2$ by furfuryl alcohol. The experiment involved an aerated solution of TFPP@MCM-41 (1.0 g L^{-1}) and FA (1×10^{-2} mol L^{-1}) which was irradiated with UV light. No significant change on the FA concentration was observed after 4 h, indicating absence of any significant singlet oxygen formation.

These results suggest that the singlet oxygen is not involved in the mechanism of photodegradation of TMP by TFPP@MCM-41 as was corroborated by the absence of any effect of the oxygen concentration on the reaction rate. In addition, it should also be noticed that no evidence of singlet oxygen phosphorescence was obtained following excitation of TFPP immobilized into MCM-41, in contrast to the results observed with the same porphyrin in homogeneous solution [18].

3.3.2. Photoinduced degradation of fenamiphos and diuron

The sensitizer that showed the best performance in the photodegradation of the TMP, TFPP@MCM-41 and the corresponding copper(II) complex, CuTFPP@MCM-41, were used to promote the photocatalytic degradation of two others pesticides, fenamiphos and diuron. The photodegradation studies were carried out under similar irradiation conditions to those used for TMP. An aqueous solution of fenamiphos (1.0×10^{-4} mol L^{-1}) containing TFPP@MCM-41 (1.0 g L^{-1}) was kept in the dark during ≈60 min, in order to reach the adsorption equilibrium between the pesticide and the catalyst. After this period the solution was irradiated in the presence, absence and saturated with oxygen. The kinetics of the photodegradation are shown in Fig. 11. It can be seen that, in contrast to the results obtained for TMP, the photodegradation of fenamiphos is clearly dependent from the oxygen concentration in solution. The photodegradation rate constant using TFPP@MCM-41 and CuTFPP@MCM-41, as photosensitizers, increase with the concentration of oxygen in the aqueous solution.

The effect of the amount of catalyst on the photodegradation rate of fenamiphos was studied within the concentration range of 0.5–3.0 g L^{-1} and the results are plotted in Fig. 12.

Complete analysis of the kinetic behaviour in this heterogeneous system must consider at least three steps, the reversible adsorption of pesticide by the MCM-porphyrin system, photoinduced degradation catalyzed by porphyrin within the MCM-41 pores, and product dissociation [53]. Detailed analysis was not attempted as it is beyond the scope of this study. However, the kinetics appear to follow pseudo-first-order behaviour, with rates increasing with the amount of catalyst, and when a large amount of TFPP@MCM-41 is present (Fig. 13) a plateau is reached, as was previously observed for TiO_2 catalyzed photodegradation of pesticides [54].

When the photolysis of fenamiphos was performed in the absence of catalyst no significant photodegradation was observed.

The herbicide fenamiphos showed 60% photodegradation in aerated solutions in the presence of TFPP@MCM-41, after 5 h irradiation. The identification of the photoproducts was made using LC–MS. The main photoproducts observed were hydroxylated fenamiphos, **2a**, with [M+1] = 320 at r_t = 10.7 min and ethylisopropylphosphoramidate, **2b**, with [M+1] = 167, arising from the P–O bond scission, at r_t = 2.85 min. An unidentified product with [M+1] = 278 appeared at r_t = 8.35 min.

The literature is scarcely in the photodegradation of fenamiphos, but in a recent study on the surface of clays and soils [55] was observed the same photoproduct (**2b**), and in another study [56] was observed the fenamiphos sulfoxide which was not found under our conditions although the photoproduct (**2a**) could be a precursor of that.

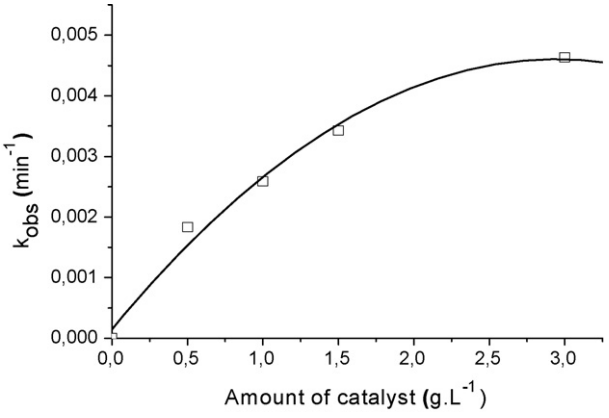

Fig. 13. Observed rate constant of the degradation of fenamiphos as function of the TFPP@MCM-41 concentration.

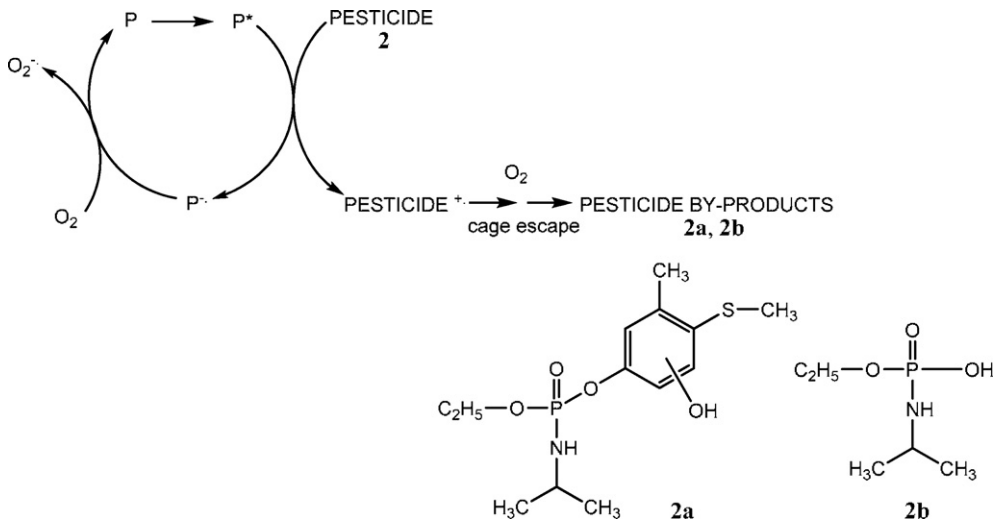

Scheme 1.

Since the presence of oxygen was found to be essential for the photodegradation of the pesticide **2** (Fig. 11) and no degradation of FA was observed in the presence of immobilized sensitizer, TFPP@MCM-41, we can suggest that the photodegradation process does not involve singlet oxygen, but probably proceeds through an electron transfer mechanism involving oxygen radical species, followed by regeneration of the photocatalyst concomitantly with the formation of superoxide anion (Scheme 1). In contrast, in the absence of oxygen, back electron transfer will occur in the cage radical ion pair to regenerate porphyrin and pesticide in their ground states.

The viability of this electron transfer process is suggested form the oxidation potentials of TMP (0.63 V) and diuron (0.80 V), both with respect to the Ag/AgCl electrode (E° = 0.22 V with respect to the *nhe*). Whilst we do not know the oxidation potential of the excited porphyrins, the energy of the lowest excited singlet state (1.91 eV) is comparable with excited TPP which as an oxidation potential $E^{\circ}(TPP_S^{*}/TPP^{-})$ = 1.05 eV with respect to the *nhe* and similar to CuTPP with an E° = 1.17 eV with respect to the *nhe*. This indicates that electron transfer will be energetically favourable.

The identification of the photogenerated products for diuron **3** was also made using LC–MS technique under similar conditions. The main photoproducts observed were the demethylated product ([3-(3,4-dichlorophenyl)-1-methylurea], **3a**, with [M+1] = 219 with r_t = 12.5 min, the 3-(3-chloro-4-hydroxyphenyl)-1,1-dimethylurea, **3b**, at r_t = 8.9 min and its isomer 3-(3-hydroxy-4-chlorophenyl)-1,1-dimethylurea, **3b′**, with [M+1] = 215 at r_t = 9.8 min. A small amount of dechlorinated compound, **3c**, was found with [M+1] = 185 at r_t = 11.4 min.

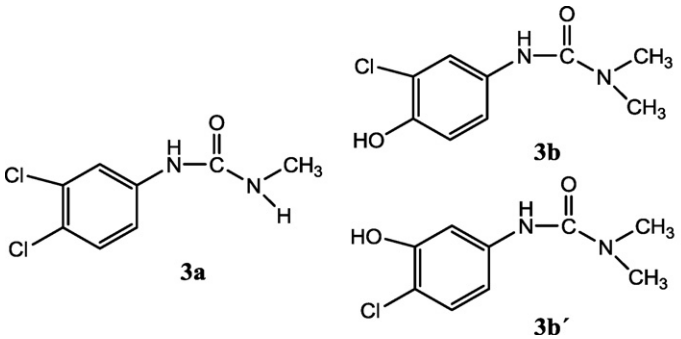

These photoproducts are in agreement with other previously reported systems involving a radical mechanism where demethylated and hydroxylated isomerized products have been observed [57–60].

3.3.3. Reuse of the immobilized catalysts

After 5 h irradiation of pesticides **1**, **2**, and **3** in the presence of TFPP@MCM-41, the solid was recovered by filtration and washed with water several times. After drying at 120 °C during 12 h, the catalyst was reused and evaluated in the photodegradation of pesticides **1**, **2** and **3**, under the same conditions. No significant decrease of the activity was observed. This system, using porphyrins immobilized into MCM-41, has a great advantage relative to the homogeneous porphyrin photocatalysts [19] where significant photodecomposition of the porphyrins was observed. We believe that this makes the system a promising candidate for water treatment and remediation.

4. Conclusions

Ship-in-a-bottle synthesis using the nitrobenzene method in the presence of MCM-41 is shown to be an efficient process to prepare porphyrins and their copper metal complexes immobilized into the silica channels, as shown by spectroscopic and thermal data.

A comparative study of the effect of the halogen atom of the immobilized porphyrins TFPP@MCM-41 and TDCPP@MCM-41 and their corresponding copper metal complexes CuTFPP@MCM-41 and CuTDCPP@MCM-41, on the photodegradation of the pesticide 2,4,6-trimethylphenol, **1**, in aerated solution shows that TFPP@MCM-41 is the most efficient photocatalyst.

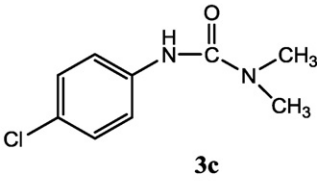

The photodegradation of aqueous solutions of the herbicide fenamiphos in the presence of TFPP@MCM-41 leads to hydroxylated fenamiphos **2a** and ethyl-isopropylphosphoramidate **2b** as the main photoproducts, and follows pseudo-first-order kinetics in an oxygen dependent process, with 10% photodegradation in deaerated solution, 60% in the presence of air and 80% in oxygen saturated solution, after 5 h irradiation.

Product analysis following diuron photodegradation with TFPP@MCM-41 using LC–MS shows that transformation on the side amine group and substitution on the aromatic ring occurs, yielding the demethylated product ([3-(3,4-dichlorophenyl)-1-methylurea] **3a**, the 3-(3-chloro-4-hydroxyphenyl)-1,1-dimethylurea **3b** and its isomer 3-(3-hydroxy-4-chlorophenyl)-1,1-dimethylurea **3b′**.

To obtain an insight on the mechanism, no photodegradation is observed when TFPP@MCM-41 is irradiated in presence of furfuryl alcohol showing the absence of singlet oxygen as an intermediate. The overall results suggest that the photodegradation of pesticides **1**, **2** and **3** proceeds *via* a radical process.

The solid TFPP@MCM-41 exhibits high photocatalytic activity for photodegradation of the pesticides **1**, **2** and **3**, and can be reused without any significant decrease in activity.

Acknowledgments

The authors thank FTC for the financial support from PTDC/QUI/66015/2006. M. Silva also thanks FCT for a post-doc grant SFRH/BPD/34372/2007.

References

[1] R. Tsao, M. Eto, in: G.H. Helz, R.G. Zepp, D.G. Crosby (Eds.), Aquatic Surface Photochemistry, Lewis Publishers, Boca Raton, FL, USA, 1994 (Chapter 11).
[2] S. Rafqah, P. Wong-Wah Chung, C. Forano, M. Sarakha, J. Photochem. Photobiol. A: Chem. 199 (2008) 297–302.
[3] H.D. Burrows, L.M. Canle, J.A. Santabella, S. Steenken, J. Photochem. Photobiol. B: Biol. 67 (2002) 71–108.
[4] O. Legrini, E. Oliveros, A.M. Braun, Chem. Rev. 93 (1993) 671–698.
[5] K.E. Djebbar, A. Zertal, N. Debbache, T. Sehili, J. Environ. Manage. 88 (2008) 1505–1512.
[6] J.-M. Herrmann, J. Disdier, P. Pichat, S. Malato, J. Blanco, Appl. Catal. B: Environ. 17 (1998) 15–23.
[7] A.A. Khodja, T. Sehili, J.-F. Pilichowski, P. Boule, J. Photochem. Photobiol. A: Chem. 141 (2001) 231–239.
[8] E. Guivarch, N. Oturan, M.A. Oturan, Environ. Chem. Lett. 1 (2003) 165–168.
[9] K. Ohshiro, T. Kakuta, T. Sakai, H. Hirota, T. Hoshino, T. Uchiyama, J. Ferment. Bioeng. 82 (1996) 299–305.
[10] P. Trebse, I. Arcon, Radiat. Phys. Chem. 67 (2003) 527–530.
[11] S.A. Naman, Z.A.-A. Khammas, F.M. Hussein, J. Photochem. Photobiol. A: Chem. 153 (2002) 229–236.
[12] C. Wang, G.-M. Yang, J. Li, G. Mele, R. Słota, M.A. Broda, M.-Y. Duan, G. Vasapollo, X. Zhang, F.-X. Zhang, Dyes Pigments 80 (2009) 321–328.
[13] B. Meunier, in: F. Montanari, L. Casella (Eds.), Metalloporphyrins Catalyzed Oxidations, Kluwer Academic, Dordrecht, 1994 (Chapter 1).
[14] S.L.H. Rebelo, M.M. Pereira, M.M.Q. Simões, M.G.P.M.S. Neves, J.A.S. Cavaleiro, J. Catal. 234 (2005) 76–87.
[15] S.L.H. Rebelo, M.M. Pereira, P.V. Monsanto, H.D. Burrows, J. Mol. Catal. A: Chem. 297 (2009) 35–43.
[16] J.M. Dabrowski, M.M. Pereira, L.G. Arnaut, C.J. Monteiro, A.F. Peixoto, A. Karocki, K. Urbańska, G. Stochel, Photochem. Photobiol. 83 (2007) 897–903.
[17] M.M. Pereira, C.J.P. Monteiro, A.V.C. Simões, S.M.A. Pinto, L.G. Arnaut, G.F.F. Sá, E.F.F. Silva, L.B. Rocha, S. Simões, S.J. Formosinho, J. Porphyr. Phthalocya. 13 (2009) 567–573.
[18] D. Murtinho, M. Pineiro, M.M. Pereira, A.M.d'A.R. Gonsalves, L.G. Arnaut, M.G. Miguel, H.D. Burrows, J. Chem. Soc., Perkin Trans. 2 (2000) 2441–2447.
[19] E. Silva, M.M. Pereira, H.D. Burrows, M.E. Azenha, M. Sarakha, M. Bolte, Photochem. Photobiol. Sci. 3 (2004) 200–204.
[20] C.J.P. Monteiro, M.M. Pereira, M.E. Azenha, H.D. Burrows, C. Serpa, L.G. Arnaut, M.J. Tapia, M. Sarakha, P. Wong-Wah-Chung, S. Navaratnam, Photochem. Photobiol. Sci. 4 (2005) 617–624.
[21] S.L.H. Rebelo, A. Melo, R. Coimbra, M.E. Azenha, M.M. Pereira, H.D. Burrows, M. Sarakha, Environ. Chem. Lett. 5 (2007) 29–33.
[22] P.R. Cooke, J.R.L. Smith, J. Chem. Soc., Perkin Trans. 1 (1994) 1913–1923.
[23] F.S. Vinhado, P.R. Martins, A.P. Masson, D.G. Abreu, E.A. Vidoto, O.R. Nascimento, Y. Iamamoto, J. Mol. Catal. A: Chem. 188 (2002) 141–151.
[24] S.L.H. Rebelo, A.R. Gonçalves, M.M. Pereira, M.M.Q. Simões, M.G.P.M.S. Neves, J.A.S. Cavaleiro, J. Mol. Catal. A: Chem. 256 (2006) 321–323.
[25] D. Pattou, G. Labat, S. Defrance, J.L. Séris, B. Meunier, New J. Chem. 13 (1989) 801–804.
[26] A.V. Borissov, V.I. Tsivenko, I.A. Myasnikov, Zh. Fiz. Khim. 63 (1991) 2540.
[27] M. Benaglia, T. Danelli, F. Fabris, D. Sperandio, G. Pozzi, Org. Lett. 4 (2002) 4229–4232.
[28] F. Bedioui, Coord. Chem. Rev. 144 (1995) 39–68.
[29] K.J. Balkus Jr., A.G. Gabrielov, J. Incl. Phenom. Mol. Recogn. Chem. 21 (1995) 159–184.
[30] S. Takagi, M. Eguchi, D.A. Tryk, H. Inoue, J. Photochem. Photobiol. C: Photochem. Rev. 7 (2006) 104–126.
[31] A. Taguchi, F. Schüth, Micropor. Mesopor. Mater. 77 (2005) 1–45.
[32] V.R. Rani, M.R. Kishan, S.J. Kulkarni, K.V. Raghavan, Catal. Commun. 6 (2005) 531–538.
[33] A. Stein, B.J. Melde, R.C. Schroden, Adv. Mater. 12 (2000) 1403–1419.
[34] J. Połtowicz, E.M. Serwicka, E.B. Gonzalez, W. Jones, R. Mokaya, Appl. Catal. A: Gen. 218 (2001) 211–217.
[35] A.K. Rahiman, K. Rajesh, K.S. Bharathi, S. Sreedaran, V. Narayanan, Appl. Catal. A: Gen. 314 (2006) 216–225.
[36] W. Gan, P.J. Dyson, G. Laurenczy, React. Kinet. Catal. Lett. 98 (2009) 205–213.
[37] H. Tanaka, T. Usui, S. Sugiyama, S. Horibe, H. Shiratori, R. Hino, J Coll. Int. Sci. 291 (2005) 465–470.
[38] G.L. Athens, R.M. Shayib, B.F. Chmelka, Curr. Opin. Colloid Interface Sci. 14 (2009) 281–292.
[39] M. Silva, M.E. Azenha, M.M. Pereira, H.D. Burrows, M. Sarakha, M.F. Ribeiro, A. Fernandes, P. Monsanto, F. Castanheira, Pure Appl. Chem. 81 (2009) 2025–2033.
[40] M. Pineiro, A.L. Carvalho, M.M. Pereira, A.M.d'A.R. Gonsalves, L.G. Arnaut, S.J. Formosinho, Chem. Eur. J. 4 (1998) 2299–2307.
[41] A.M.d'A.R. Gonsalves, J.M.T.B. Varejao, M.M. Pereira, J. Heterocycl. Chem. 28 (1991) 635–640.
[42] A.K. Rahiman, K.S. Bharathi, S. Sreedaran, K. Rajesh, V. Narayanan, Inorg. Chim. Acta 362 (2009) 1810–1818.
[43] M.-Y. Chang, Y.-H. Hsieh, T.-C. Cheng, K.-S. Yao, M.-C. Wei, C.-Y. Chang, Thin Solid Films 517 (2009) 3888–3891.
[44] C.J. Medforth, Z. Wang, K.E. Martin, Y. Song, J.L. Jacobsen, J.A. Shelnutt, Chem. Commun. (2009) 7261–7277.
[45] M.M. Pereira, C.J.P. Monteiro, A.F. Peixoto, in: O.A. Attanasi, D. Spinelli (Eds.), Targets Heterocyclic Systems. Chemistry and Properties, vol. 12, Italian Society of Chemistry, Bologna, 2009, p. 258.
[46] A.D. Adler, F.R. Longo, J. Finarelli, J. Goldmacher, J. Assour, J. Org. Chem. 32 (1967) 476.
[47] T.D. Lash, Chem. Eur. J. 2 (1996) 1197–1200.
[48] F. Liu, K.L. Cunningham, W. Uphues, G.W. Fink, J. Schmolt, D.R. McMillin, Inorg. Chem. 34 (1995) 2015–2018.
[49] G.W. Hodgson, E. Peterson, B.L. Baker, Mikrochim. Acta 57 (1969) 805–814.
[50] N. Toyama, M.A. Someda, T. Ichino, Y. Kaizu, J. Phys. Chem. A 104 (2000) 4857–4865.
[51] K.L. Cunningham, K.M. McNett, R.A. Pierce, K.A. Davis, H.H. Harris, D.M. Falck, D.R. McMillin, Inorg. Chem. 36 (1997) 608–613.
[52] H. Grasdalen, J. Magn. Reson. 9 (1973) 166–174.
[53] M.A. Zanjanchi, A. Ebrahimian, M. Arvand, J. Hazard. Mater. 175 (2010) 992–1000.
[54] S. Rafqah, P. Wong-Wah Chung, A. Aamili, M. Sarakha, J. Mol. Catal. A: Chem. 237 (2005) 50–59.
[55] L. Tajeddine, M. Nemmaoui, H. Mountacer, A. Dahchour, M. Sarakha, Environ. Chem. Lett. 8 (2010) 123–128.
[56] D. Barceló, G. Durand, N. De Bertrand, Toxicol. Environ. Chem. 38 (1993) 183–199.
[57] K. Macounová, H. Krýsová, J. Ludvík, J. Jirkovský, J. Photochem. Photobiol. A: Chem. 156 (2003) 273–282.
[58] J. Jirkovský, V. Faure, P. Boule, Pestic. Sci. 50 (1997) 42–52.
[59] M.C. Edelahi, N. Oturan, M.A. Oturan, Y. Padellec, A. Bermond, K. El Kacemi, Environ. Chem. Lett. 1 (2004) 233–236.
[60] M.C. López, M.I. Fernández, S. Rodríguez, J.A. Santaballa, S. Steenken, E. Vulliet, Chem. Phys. Chem. 6 (2005) 2064–2074.